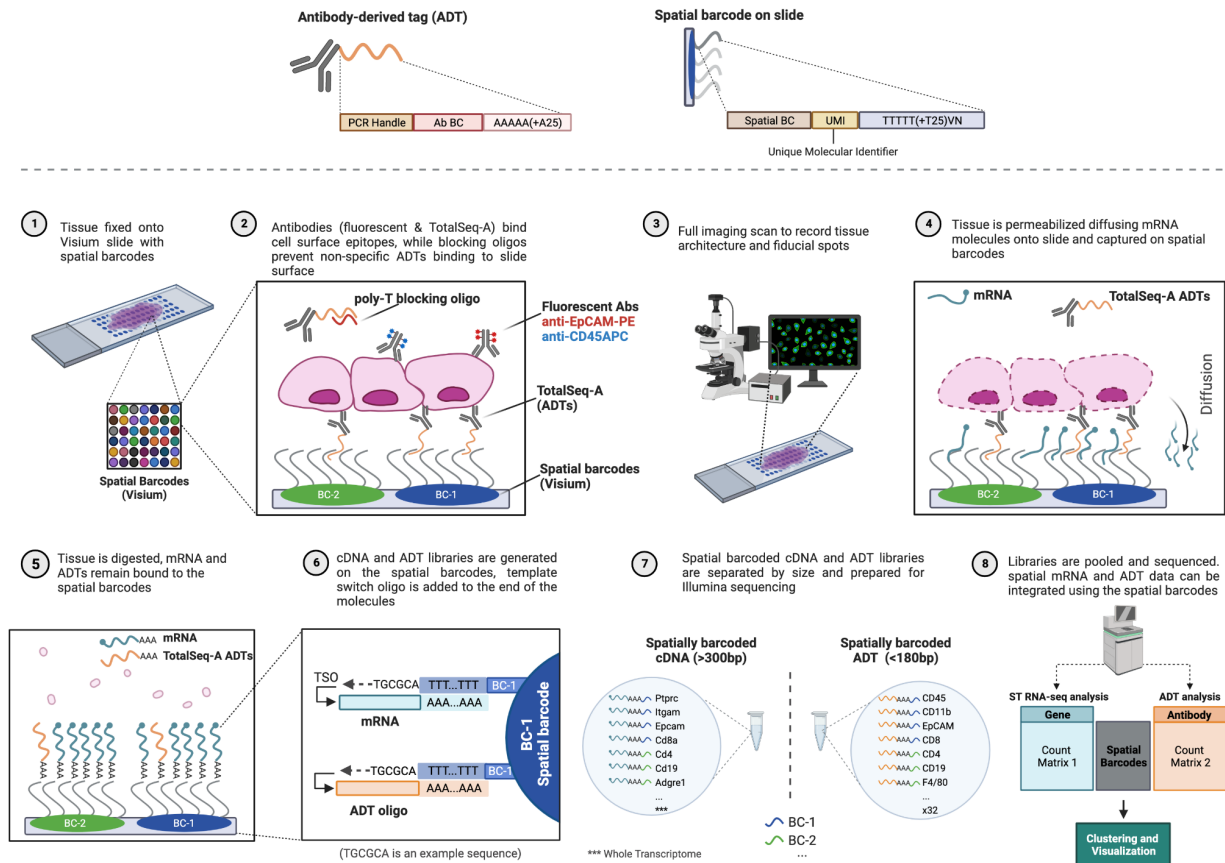


SPOTS (Spatial PRotein and Transcriptome Sequencing) Workflow



Supplementary Figure 1: Workflow schematic of SPOTS

(Step 1) Tissue sections are mounted onto Visium slide, fixed for 10 min, and immunostained **(Step 2)** with fluorescent and TotalSeq-A antibodies (same clones) for 90 min in the presence of poly-T blocking oligos that prevent non-specific ADTs binding to slide surface. After washes, tissue is scanned under a scanning microscope to capture the tissue structure and fiducial spots **(Step 3)**. The tissue is then permeabilized **(Step 4)**, and RNA diffuses onto the poly-T oligos on the spatial barcodes. Following tissue digestion **(Step 5)**, and template switched RT-PCR **(Step 6)**, gene expression and ADT libraries are generated to preserve associated spatial barcodes and RNA sequence/ADT antibody barcodes **(Step 7)**. Gene expression and ADT libraries are sequenced, and data are integrated using our designated pipeline **(Step 8)**.

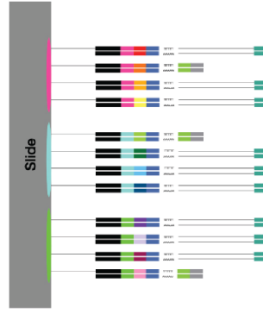
a



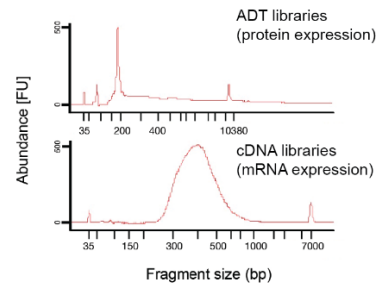
b



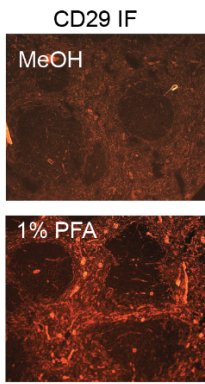
c



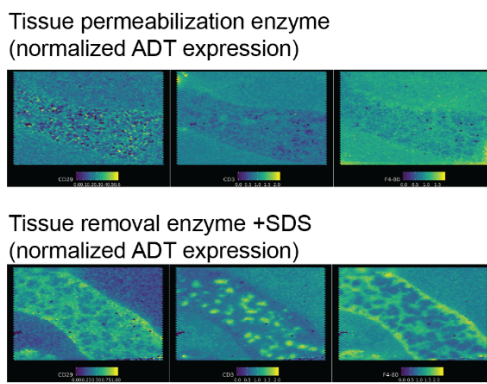
d



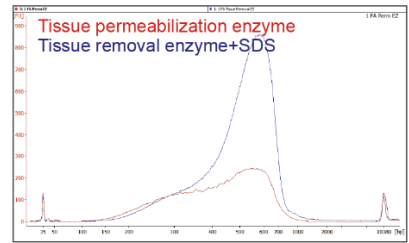
e



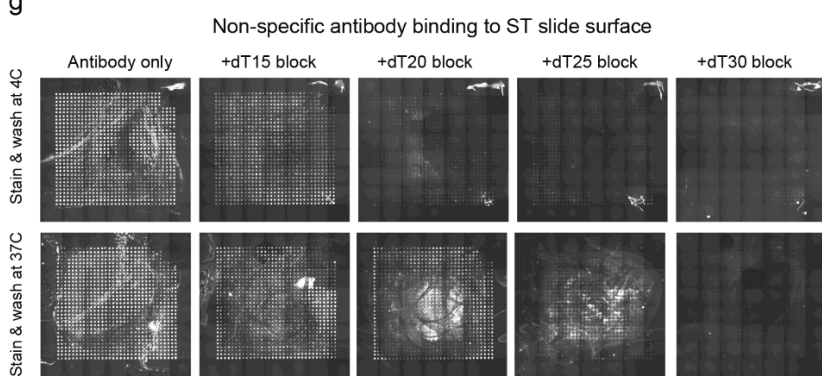
f



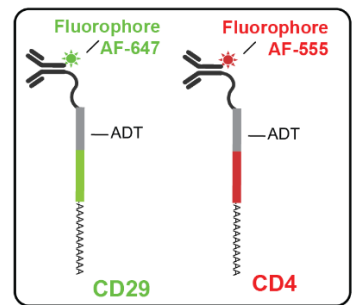
cDNA libraries (mRNA expression)



g

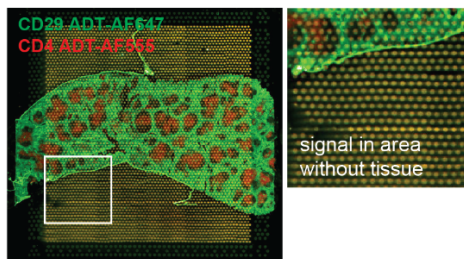


Dual tagged antibodies (ADT+fluorophore)

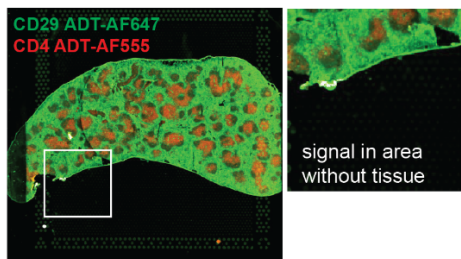


h

without poly-dT blocking aligos



with poly-dT blocking aligos



Supplementary Figure 2: SPOTS library preparation and optimizations.

(a) Illustration of the structure of a barcoded oligo, including Read 1, spatial barcode (SB), unique molecular identifier (UMI), and poly-T (T_{30}) sequences, attached to the Visium slide.

(b) Illustration of the structure of an ADT-conjugated antibody, including a PCR handle (Handle), an antibody barcode (AB), and poly-A (A_{30}).

(c) Schematic of SPOTS following second strand synthesis. ADT and mRNA location is recorded through spatial barcodes on the Visium slide.

(d) After cDNA amplification, ADT and cDNA libraries can be separated and prepared for sequencing to produce indexed ADTs (top panel, BioA) and gene expression libraries (bottom panel, BioA).

(e) IF analysis using CD29 antibodies (TotalSeq-A clone) in spleen tissues that were fixed for 10 min at 25°C using 100% MeOH (top) or 1% PFA (bottom).

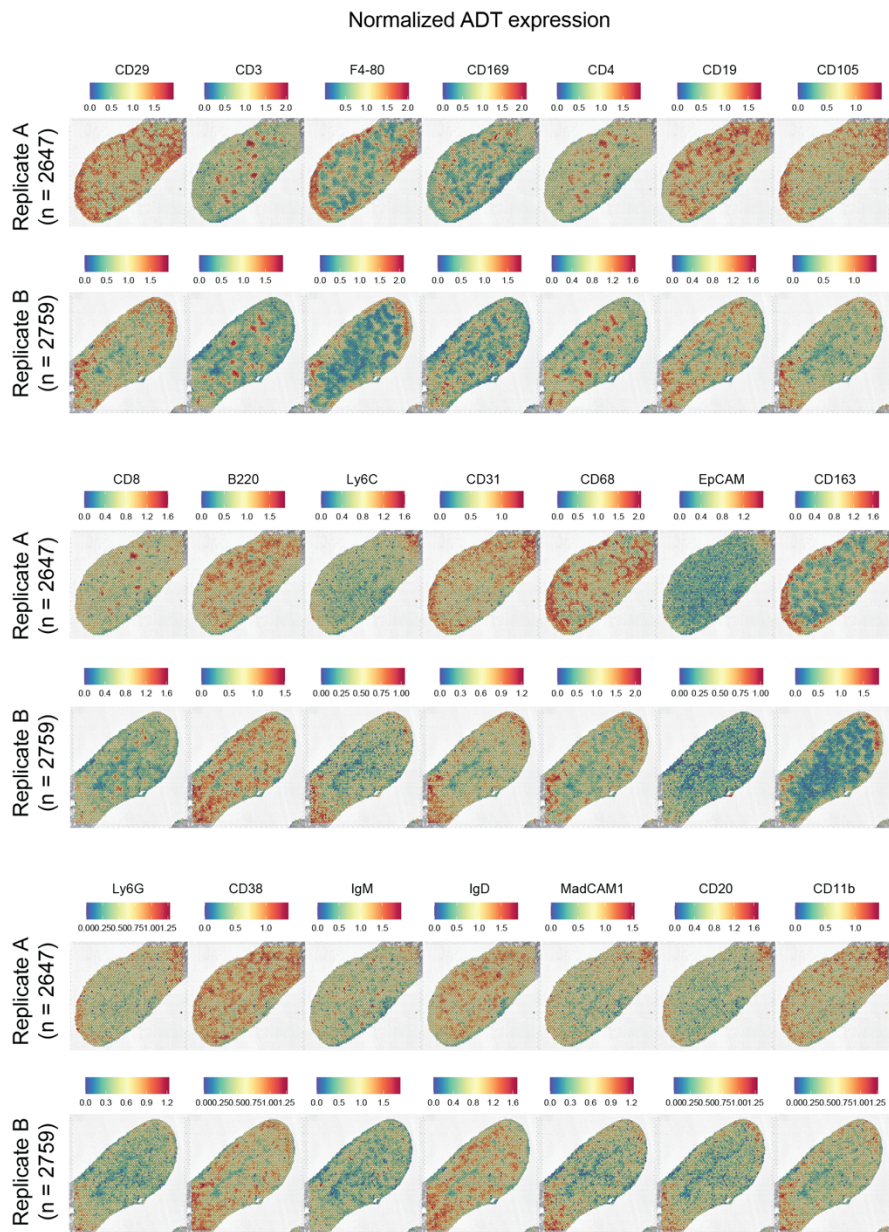
(f) Normalized ADT levels (left) and cDNA libraries (right, BioA) of indicated antibodies using tissue permeabilization vs. tissue removal enzyme and SDS.

(g) Poly-T blocking oligo length and wash temperature titration. Titration of different poly-T blocking oligo lengths and their ability to hinder binding of dual-tagged antibodies

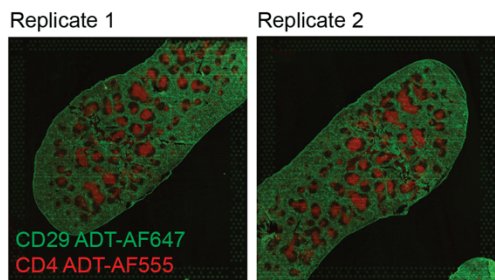
(ADT+fluorophore) to poly-A surface probes at either 4°C or 37°C. Note the difference between the different temperatures for dT20.

(h) IF using dual-tagged antibodies (ADT+fluorophore) of CD29 (green) and CD4 (red) in mouse spleens in the presence or absence of 20µM poly-T blocking oligos. Note for reduction of non-specific bindings in tissue-free areas.

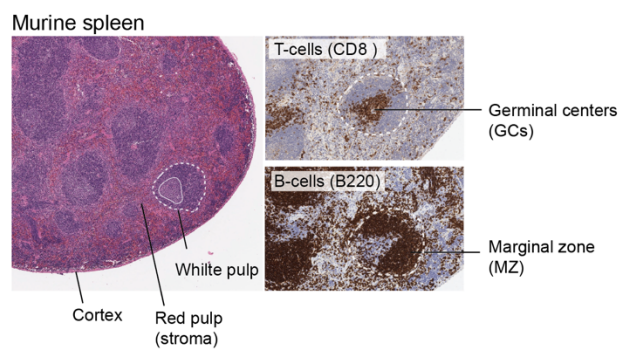
a



b



c



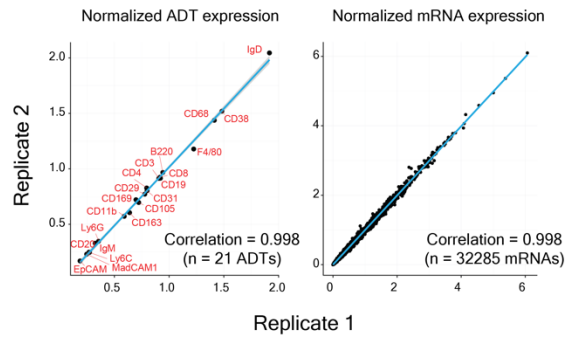
Supplementary Figure 3: Normalized ADT levels in spleens.

(a) Normalized ADT levels of all 21 surface proteins in two spleen samples.

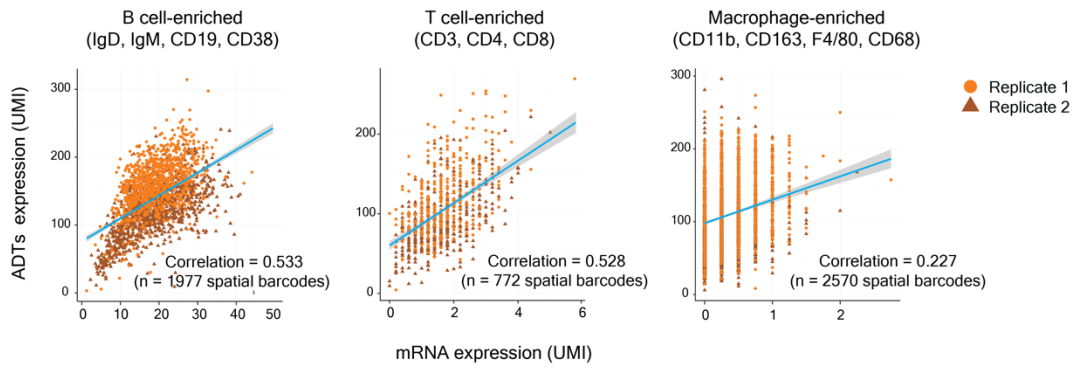
(b) Immunofluorescence staining for CD29 (green) and CD4 (red) in spleen tissues from **a**, using fluorophore-ADT dual-tagged antibodies.

(c) Serial histological sections of mouse spleen (unstimulated) stained for H&E, B cells (B220), and T cells (CD8), demonstrating the typical spatial cell organization.

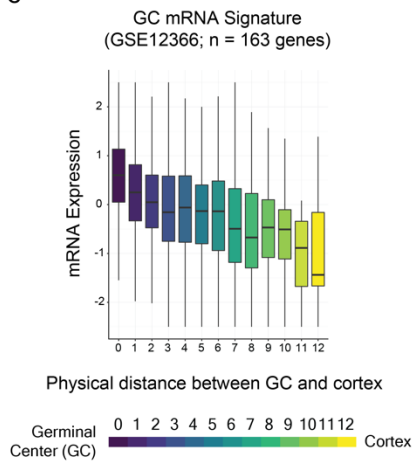
a



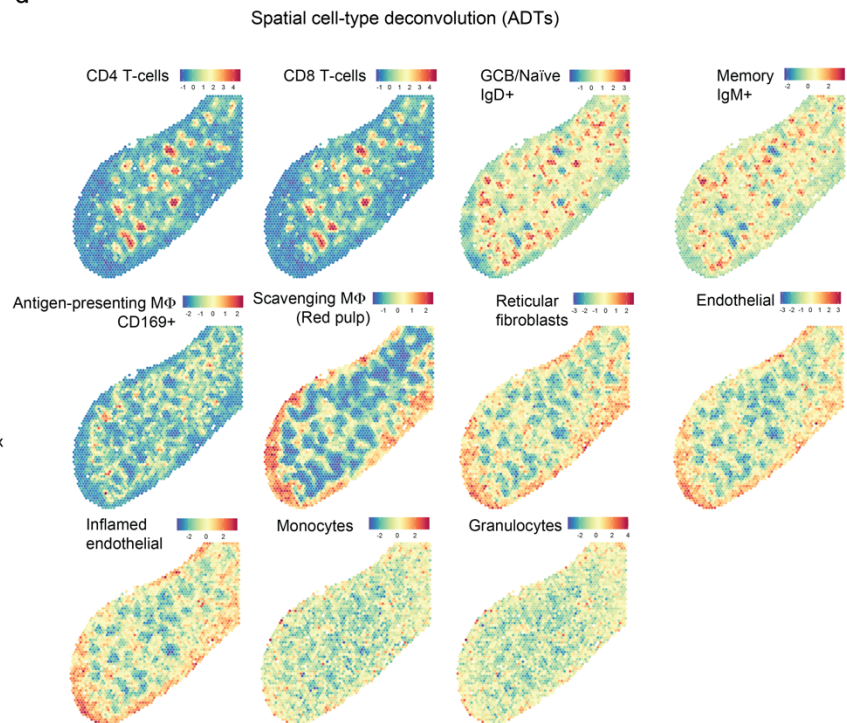
b



c



d



Supplementary Figure 4: Reproducibility and quality controls of SPOTS spleen data.

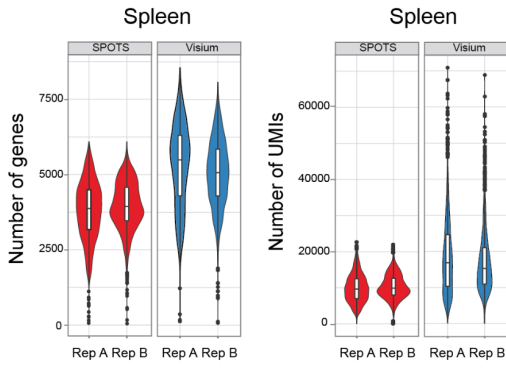
(a) Correlation of normalized ADT levels and mRNA expressions between two biological replicates of mouse spleen.

(b) Correlation between mRNA and different ADT levels (UMI) at single spatial barcode level for B cell, T cell, and macrophage enriched clusters across spatial barcodes in two biological replicates.

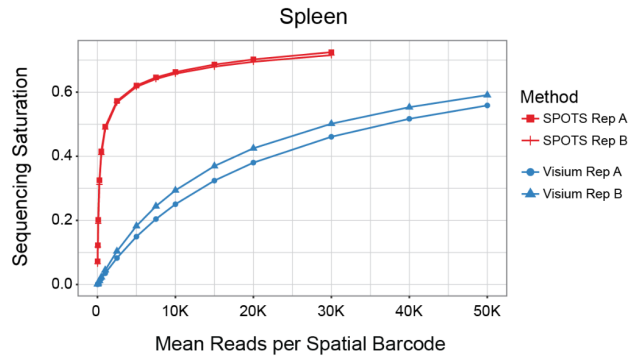
(c) Boxplot showing mRNA expression levels of germinal center (GC) specific genes (GSE12366; n = 163 genes) as a function of the distance from the center of GCs. The boxes were colored by the physical distance from the center of GCs as shown in **Fig. 1f**.

(d) Cell-type deconvolution based on ADTs (Z-score) of each spatial barcode overlaid onto the spleen tissue. Magnified areas are shown in **Fig. 1h**.

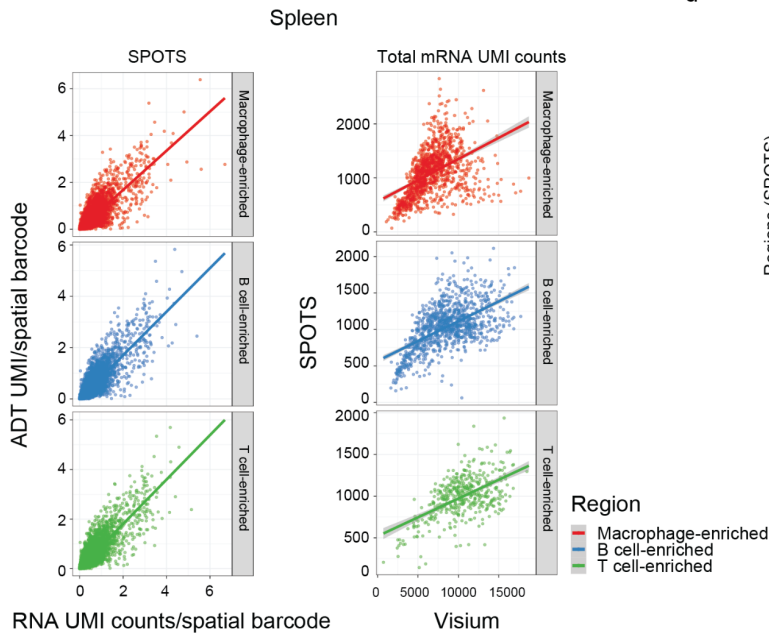
a



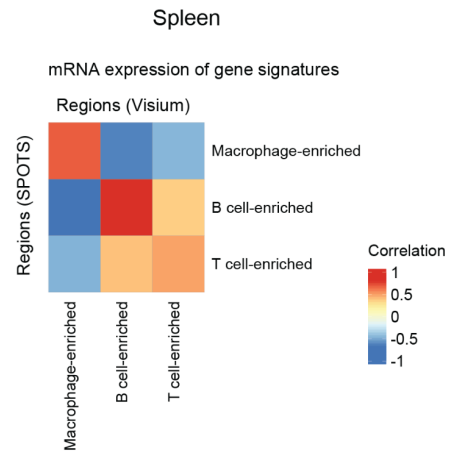
b



c



d



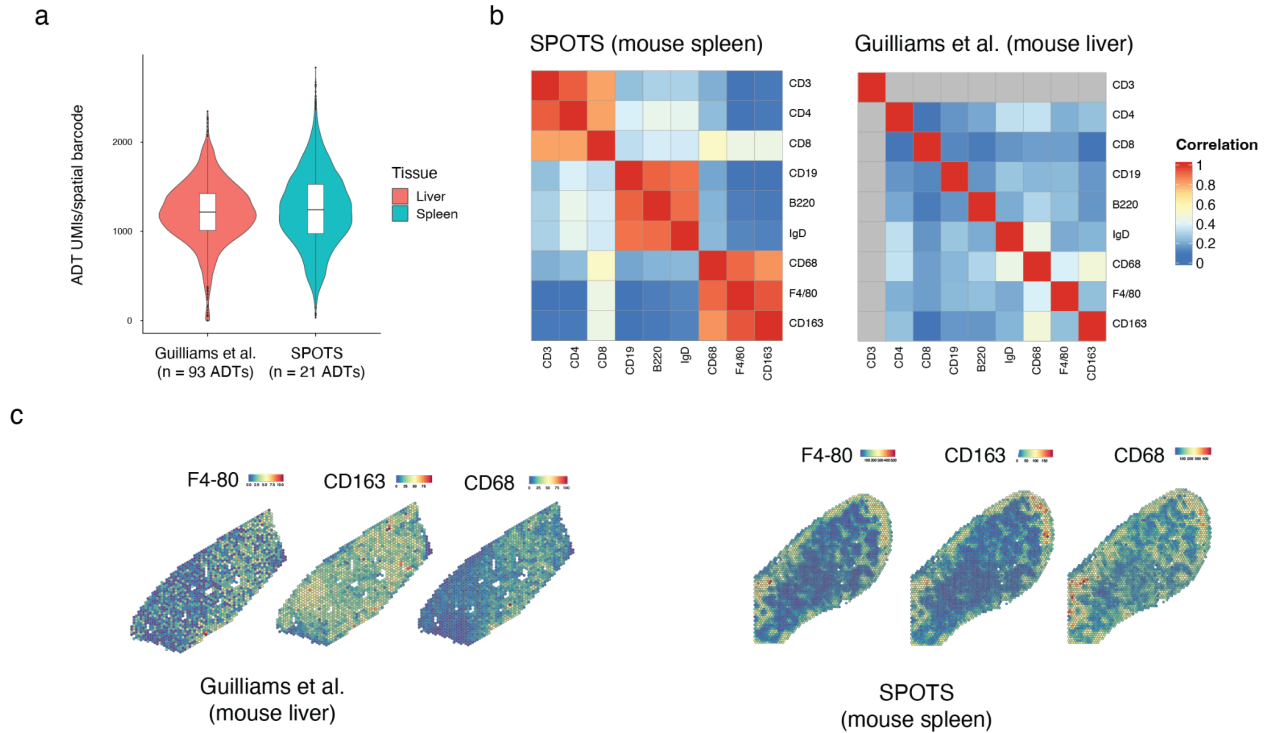
Supplementary Figure 5: Comparative performance analysis between SPOTS and Visium alone in spleen

(a) Total detected genes and UMIs across spatial barcodes in biological replicates of spleens using SPOTS or Visium alone (n=2 each). Sequencing depth: SPOTS rep A ~175K reads per spot, SPOTS rep B ~155K reads per spot, Visium rep A ~124K reads per spot, Visium rep B ~110K reads per spot.

(b) Sequencing saturation curves for RNA of the two replicates of mouse spleen using SPOTS or Visium alone.

(c) Correlation between mRNA and ADT UMI counts (left panel) in spleens using SPOTS. Correlation of total mRNA UMI counts in spatial barcodes using SPOTS (Y-axis) and Visium only (X-axis).

(d) Correlation of gene expression signatures in the indicated cell clusters as detected by SPOTS (Y-axis) and Visium alone (X-axis).



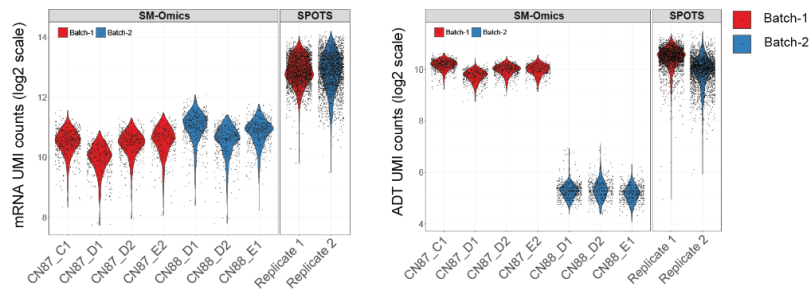
Supplementary Figure 6: Performance comparison of SPOTS to Guilliams et al.

(a) Total ADT UMI counts across the tissue spatial barcodes using 93 or 21 TotalSeq-A antibodies (Guilliams in mouse liver or SPOTS in mouse spleen, respectively).

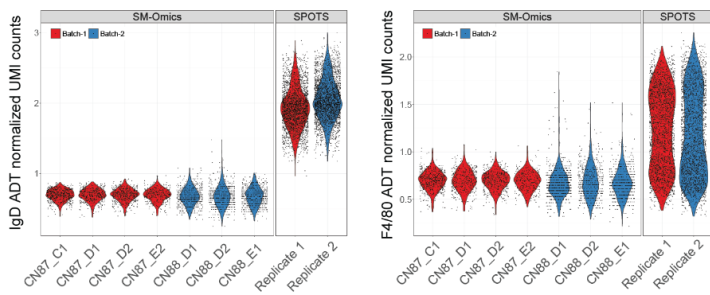
(b) Correlation map between several ADT markers of the same cell type in mouse liver (Guilliams et al.) and mouse spleen (SPOTS). ADTs: T cells (CD8, CD4, CD3), B cells (CD19, B220, IgD), and macrophages (F4/80, CD68, CD163).

(c) Visualization of normalized ADTs of macrophages from panel b in liver (Guilliams et al.) and spleen (SPOTS).

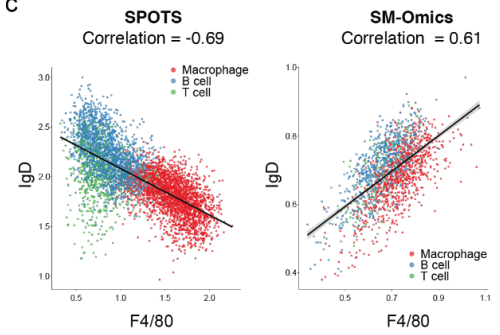
a



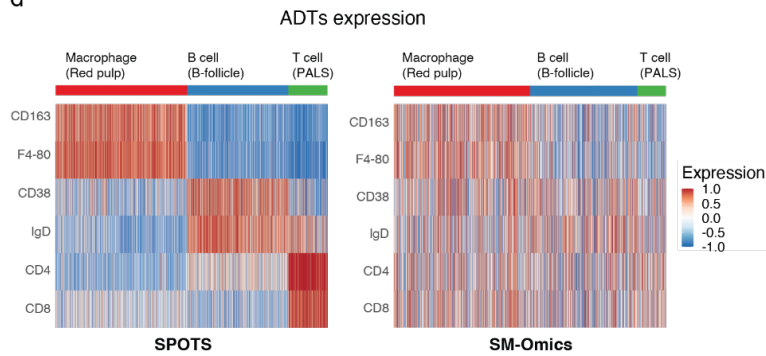
b



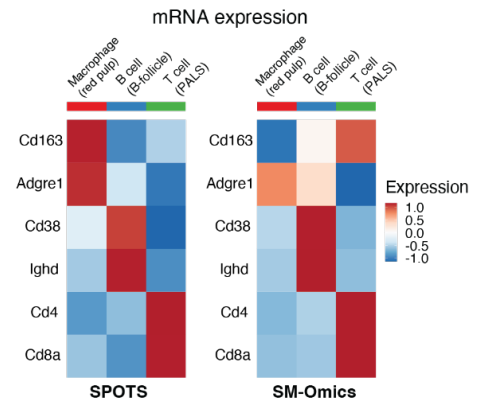
c



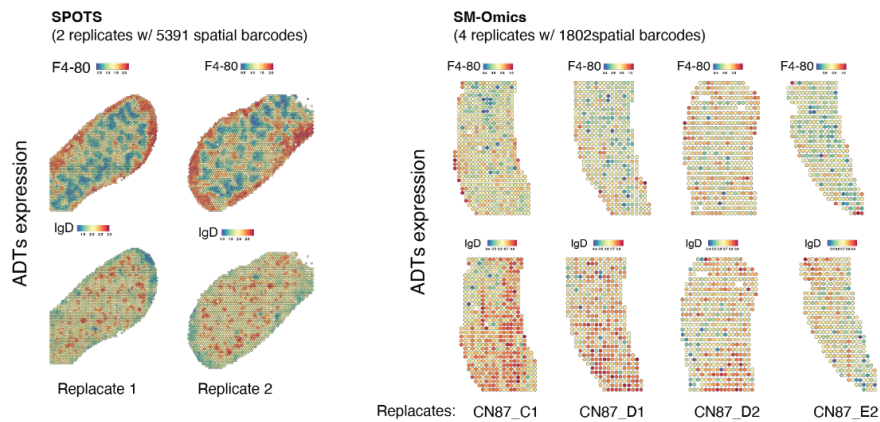
d



e



f

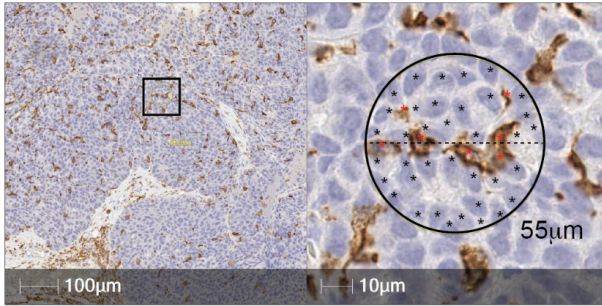


Supplementary Figure 7: Performance comparison of SPOTS to SM-Omics.

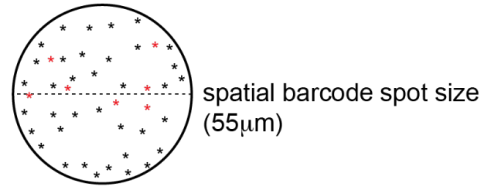
- (a) Total mRNA and ADT counts across spatial barcodes in biological replicates of spleens.
- (b) Total ADT counts of F4/80 (macrophages) and IgD (B cells) across biological replicates of spleens.
- (c) Correlations between IgD and F4/80 (normalized ADT counts) for each spatial barcode in splenic tissues by SPOTS and SM-Omics. Note the anti-correlation between F4/80+ macrophage-enriched (Red pulp) and IgD+ B cell-enriched (B follicle) regions in the SPOTS analyses.
- (d) Differentially expressed ADT levels (Z-score) for each cluster of spatial barcodes in splenic tissues. Left panel: SPOTS, right panel: SM-Omics
- (e) Heatmap showing differentially expressed mRNAs (Z-score) in each cluster of spatial barcodes in splenic tissues. Left panel: SPOTS, right panel: SM-Omics
- (f) Visualization of normalized ADT expression of macrophages (F4/80) and B-cells (IgD) in spleens using SPOTS (left) and SM-Omics (right).

a

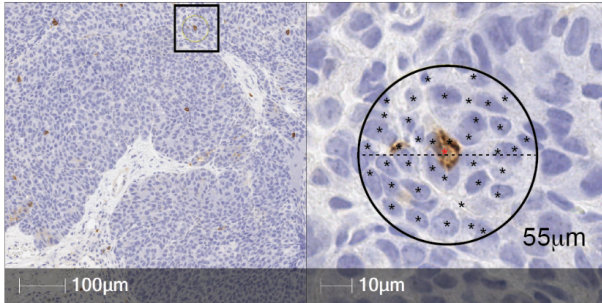
IBA-1 IHC (Macrophages)



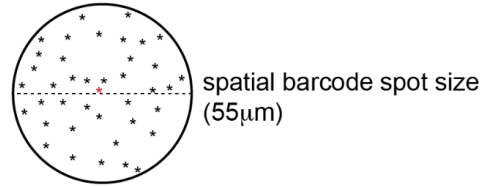
Macrophages abundance



CD8 IHC (T-cells)

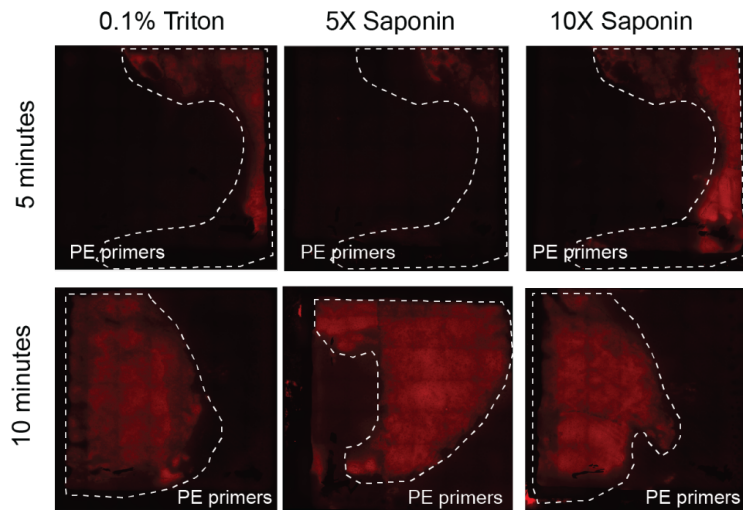


T-cells abundance



b

Tissue permeabilization methods
(Breast cancer tissue; MMTV-PyMT model)

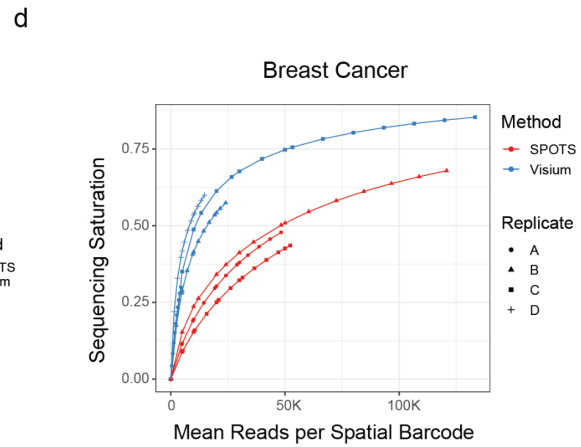
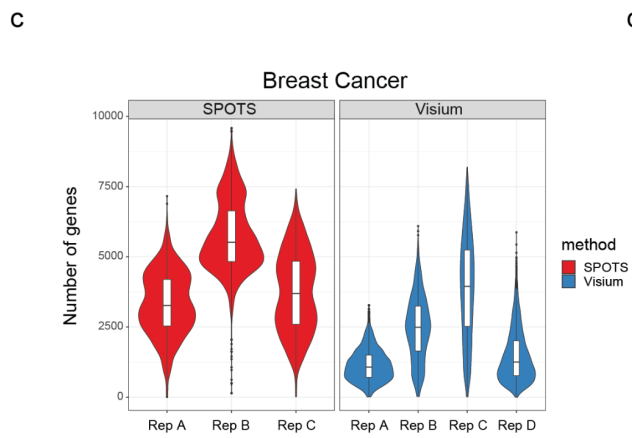
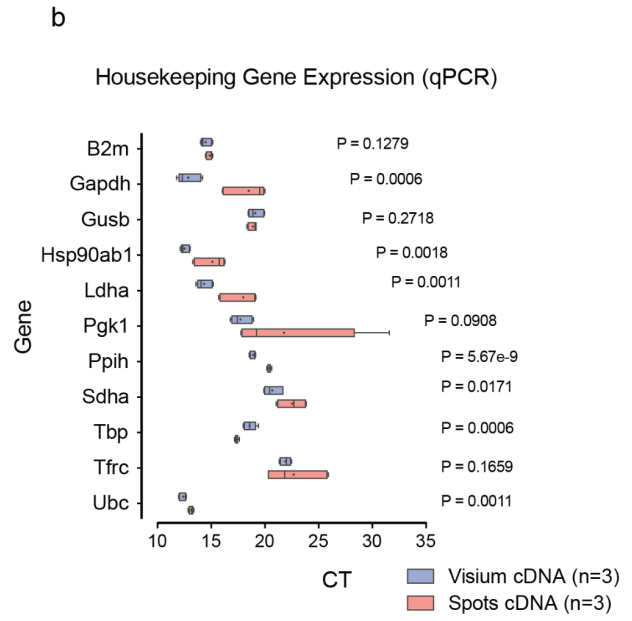
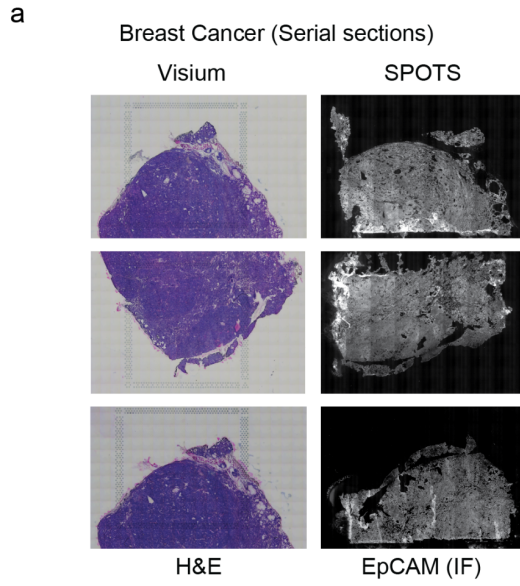


----- tissue outline

Supplementary Figure 8: Breast cancer tissue architecture and optimizations

(a) Immunohistochemistry (IHC) analysis of CD8 (T cells) and IBA-1 (macrophages) in mammary tumor section from MMTV-PyMT model demonstrating the typical abundance of T cells and tumor-associated macrophages in breast tumors.

(b) Fluorescence imaging of TRITC labeled cDNA from mouse breast tumors following 5 or 10 minutes with 5X or 10X saponin or 0.1% Triton pre-staining permeabilization conditions. Dotted lines outline tissue borders.



Supplementary Figure 9: Gene expression analysis of housekeeping genes in SPOTS and Visium cDNA libraries and comparative performance analysis between SPOTS and Visium-alone in breast cancer tissue.

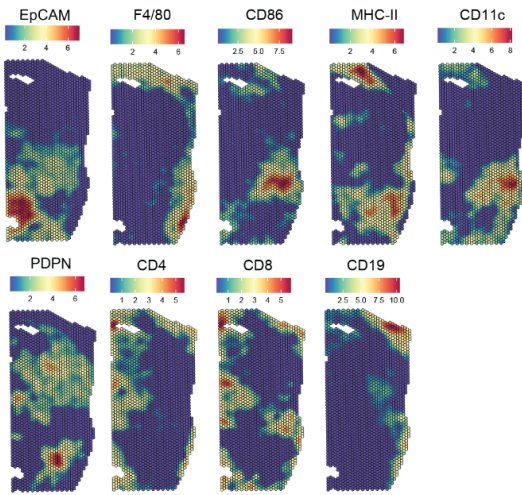
(a) Images of serial sections of 3 biological replicates of mammary tumors using Visium protocol (H&E staining images) or SPOTS protocol (IF images of EpCAM).

(b) Gene expression cycle threshold (CT) values of the indicated housekeeping genes using cDNA generated by Visium or SPOTS protocols from **panel a**.

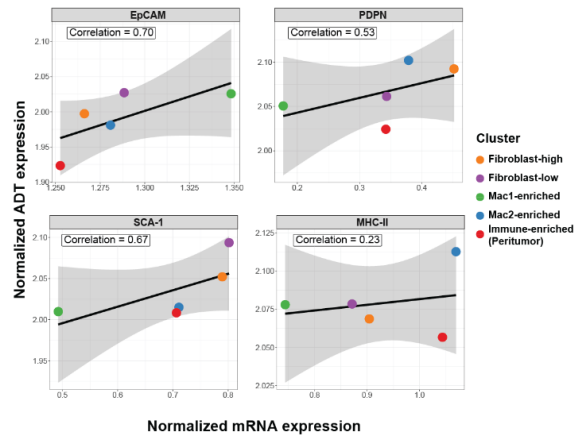
(c) Total detected genes across spatial barcodes in biological replicates of mammary tumors using SPOTS (n=3) or Visium alone (n=4). Sequencing depths for all Visium and SPOTS samples ~50K reads per spot.

(d) Sequencing saturation curves for RNA of the biological replicates from **panel c**.

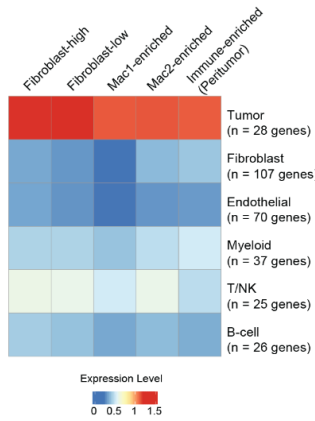
a



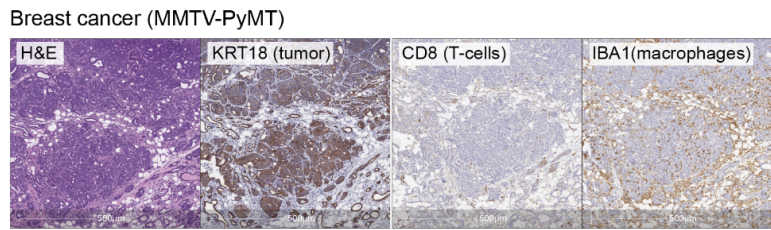
b



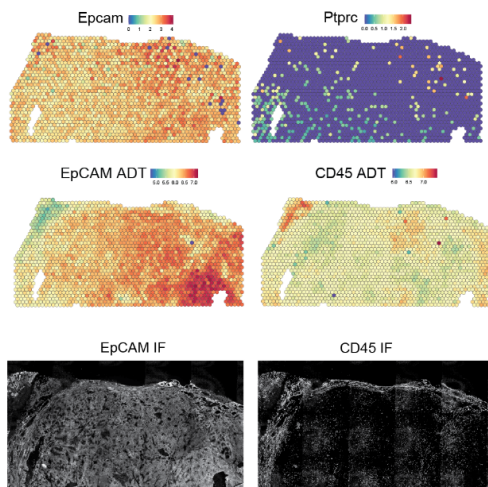
c



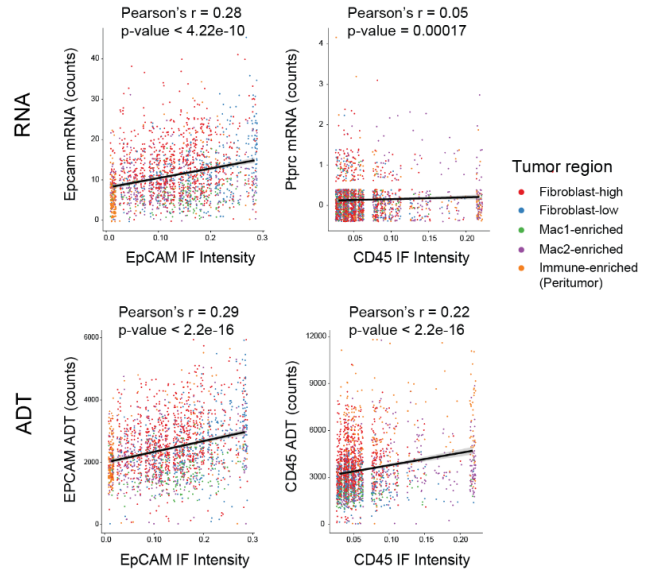
d



e



f



Supplementary Figure 10: Spatial mRNA and ADT levels in breast cancer TME.

(a) Normalized ADT levels (Z-score) of selected markers in a tissue section of MMTV-PyMT breast cancer.

(b) Correlation between normalized mRNA expression and ADT levels of the indicated surface markers (EpCAM, PDPN, SCA-1, MHC-II). Pearson's correlation coefficients were calculated on cluster level and are indicated in the boxed labels.

(c) Average normalized mRNA expressions of key cell-type marker genes (GSE158677) in each spatial cluster.

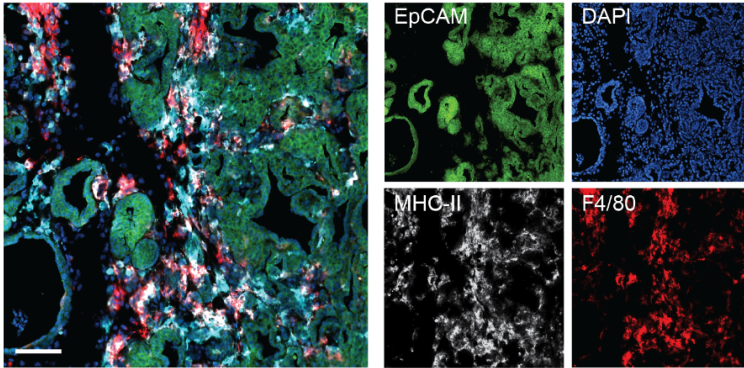
(d) H&E staining and IHC analysis of KRT18 (tumor cells), CD8 (T cells), and IBA1 (macrophages) in serial sections of the MMTV-PyMT breast cancer model, demonstrating the typical abundances of tumor cells, T cells, and macrophages in mammary tumors. Scale bar 500 μ m.

(e) Normalized mRNA and ADT expression levels of Epcam and Ptprc along with their corresponding IF signals in breast cancer tissue.

(f) Pearson's correlation analysis between total UMI mRNA or UMI ADT counts and IF intensities of the indicated genes across the spatial barcodes. Pearson's correlation coefficients are shown; mRNA/IF (top) and ADT/IF (bottom).

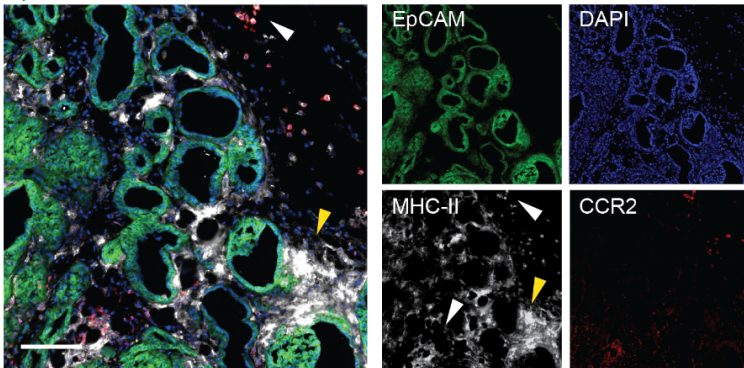
a

EpCAM MHC-II F4/80 DAPI



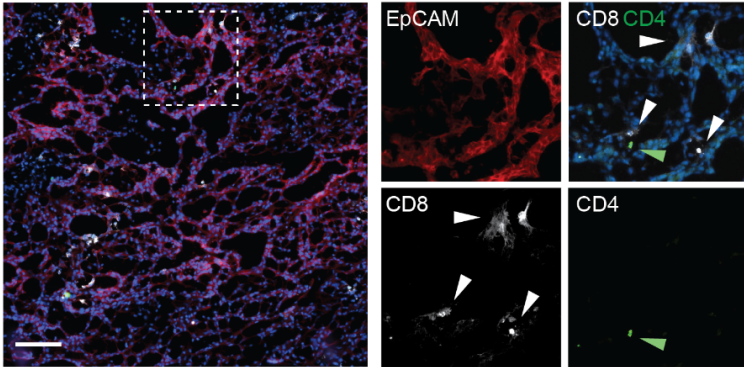
b

EpCAM MHC-II CCR2 DAPI



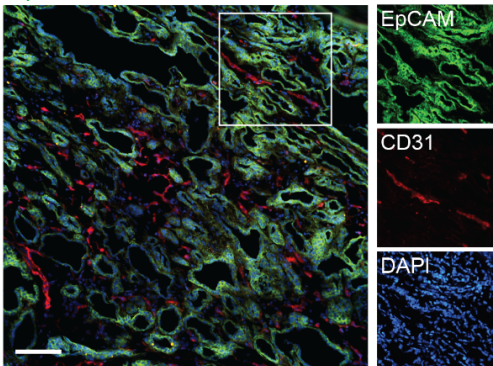
c

CD4 CD8 EpCAM DAPI



d

EpCAM CD31 DAPI



Supplementary Figure 11: IF analysis using TotalSeq-A clones in breast cancer.

(a) IF analysis of EpCAM and DAPI to visualize tissue architecture along with F4/80 and MHC-II to highlight tumor-associated macrophages (TAMs). Scale bar 500 μ m.

(b) IF analysis of EpCAM and DAPI to visualize tissue architecture along with CCR2 and MHC-II to highlight two populations of TAMs (MHC-II+ CCR2-/MHC-II+ CCR2+). Scale bar 500 μ m.

(c) IF analysis of EpCAM and DAPI to visualize tissue architecture along with CD4 and CD8 to mark the two populations of tumor-infiltrating T cells. Scale bar 500 μ m.

(d) IF analysis of EpCAM and DAPI to visualize tissue architecture and CD31 to visualize blood vessels. Scale bar 500 μ m.

Supplementary table legends

Supplementary Table 1. ADT sequences, primers, and indices were used in this study.

Supplementary Table 2. Spleen metadata. **Tab 1:** Metadata for each spatial barcode of the spleen tissues. **Tab 2:** ADT deconvolution results for each spatial barcode of the spleen tissues.

Tab 3: Distance between the germinal centers and spleen cortex for each spatial barcode of the analyzed spleens.

Supplementary Table 3. Spleen differential expression analysis results. **Tab 1:** Differentially expressed ADTs in the spleen tissues. **Tab 2:** Differentially expressed mRNAs in the spleen tissues.

Supplementary Table 4. Breast cancer metadata. **Tab 1:** Metadata for each breast cancer spatial barcodes. **Tab 2:** ADT deconvolution results for each breast cancer spatial barcodes. **Tab 3:** Transcriptome deconvolution results for each breast cancer spatial barcodes. **Tab 4:** ADT and mRNA modality weights for each breast cancer spatial barcodes. **Tab 5:** EpCAM and CD45 immunofluorescent signal intensities for each breast cancer spatial barcodes.

Supplementary Table 5. Breast cancer differential expression analysis results. **Tab 1:** Differentially expressed ADTs in the breast cancer tissues. **Tab 2:** Differentially expressed mRNAs in the breast cancer tissues. **Tab 3:** GSE158977 differentially expressed genes. **Tab 4:** Differentially expressed genes between Mac1-enriched and Mac2-enriched regions in breast cancer tissue.